

A new method to clarify contribution of chiral magnetic effect in small collision system $p^\uparrow + A$ involving a transversely polarized proton

Gui-Zhen Wu (吴桂珍),^{1,*} Zong-Wei Zhang (张宗炜),^{2,1,*} Chen Gao (高晨),¹ Yi Xu (许易),¹ and Wei-Tian Deng (邓维天)^{1,†}

¹*School of Physics, Huazhong University of Science and Technology, Wuhan 430074, China*

²*Modern Industrial School of Health Management, Jinzhou Medical University, Jinzhou 121000, China*

In this paper, we propose a new experiment method to check contribution of chiral magnetic effect (CME). With experimental data of DIS involving transversely polarized proton, we have calculated the 3-D charge density inside the polarized proton, which is found to have a significant violation to spherical symmetry. Then we have calculated the property of electromagnetic field (E-M field) generated by a single transversely polarized proton (p^\uparrow). Based on them, the E-M field generated in small collision system $p^\uparrow + A$ are studied. We find that the orientation of this E-M field has a significant dependence on the polarization direction of the proton, and the correlator ($\Delta\gamma$) has also significant dependence on the angle between reaction plane and polarization direction. As background contribution are canceled comparing two collision geometry schemes, only contribution of CME is remained.

In recent years, it has been recognized that there may be a CP violation effect[1–6] due to the quantum anomalous fluctuation of QCD vacuum. This effect can be observed as chiral magnetic effect (CME) in quark-gluon plasma (QGP) with existing a strong magnetic fields[3, 4]. In high energy heavy ion collision experiment, QGP is produced since the extreme environment needed for phase transition is satisfied, and a strong magnetic field is also produced in non-central heavy ion collision [7–14]. So heavy ion collision is an excellent place to study CME. A charge asymmetry (charge separation) along magnetic field is induced by the CME, which provide a way to study the quantum anomaly of QCD vacuum topology.

In order to study the charge separation, a three-point correlator γ is introduced[15]

$$\gamma_{\alpha\beta} = \langle \cos(\Phi_\alpha + \Phi_\beta - 2\Phi_{RP}) \rangle \quad (1)$$

Where Φ_α and Φ_β are azimuthal angles of charged particle α and β , Φ_{RP} is the azimuthal angle of reaction plane

respective to Lab frame. To cancel charge-independent backgrounds, the difference of correlator $\Delta\gamma = \gamma_{OS} - \gamma_{SS}$ is used[5], where γ_{OS} represents for opposite charge particle pair, γ_{SS} represents for same charge particle pair. The contribution of CME into correlator can be expressed as[16, 17]

$$\Delta\gamma_{CME} \propto B^2 \cdot \cos[2(\Phi_B - \Phi_{RP})], \quad (2)$$

where Φ_B is the azimuthal angle of magnetic field. However, a large amount of QCD background effects are also included in $\Delta\gamma$ which is related to QGP flow v_2 [18–23]. It's a huge challenge to clarify the contributions of CME and background correspondingly in experiment data of $\Delta\gamma_{exp}$.

$$\Delta\gamma_{exp} = \Delta\gamma_{CME} + \Delta\gamma_{BG}. \quad (3)$$

In this paper, we propose a new method to check and clarify the contribution of CME in small collision system involving a transversely polarized proton $p^\uparrow + A$

In our previous work[24], employing a physical Charge-Profile model to describe the inner charge distribution of a proton, we calculated the property

* These authors contribute equally to this work.

† The corresponding author; dengwt@hust.edu.cn

of electromagnetic field produced in small system p+A. We find that there is a significant azimuthal correlation between Φ_B and Φ_{RP} . Here, we forward our study to transversely polarized proton.

In DIS onto transversely polarized nucleon experiment[25], the plane charge distribution of a polarized proton is given

$$\rho_T^N(b) = \rho_0^N(b) - \sin(\phi_b - \phi_S) \int_0^\infty \frac{dQ}{2\pi} \frac{Q^2}{2M_N} J_1(bQ) \frac{G_M(Q^2) - G_E(Q^2)}{1 + \tau}. \quad (4)$$

The first term in it is the plane charge distribution of unpolarized proton, which is also given by DIS experiment [26]

$$\rho_0^N(b) = \int_0^\infty \frac{dQ}{2\pi} Q J_0(bQ) \frac{G_E(Q^2) + \tau G_M(Q^2)}{1 + \tau}. \quad (5)$$

where $\tau = \frac{Q^2}{4M^2}$, M is the mass of proton, J_0 and J_1 are cylindrical Bessel functions. The electric form factor G_E and magnetic form factor G_M of proton are given in the following parameterized form [27–29] :

$$G_E, \frac{G_M}{\mu_p} = \frac{1 + \sum_{i=1}^n a_i^{E,M} \tau^i}{1 + \sum_{i=1}^{n+2} b_i^{E,M} \tau^i}. \quad (6)$$

With these parameterization, the plane charge density of a proton polarized along $+x$ direction is shown in Fig1. we can see that the center of charge moved along $-y$ direction.

With this plane charge distribution in a polarized proton, we can derive its 3-dimensional charge profile using the same method in [24]. Shown in Fig2, we compare the 3-D charge profile of a polarized proton and an unpolarized proton. Their difference defined as $\rho_{pol} - \rho_{unpol}$, also shown in this figure. We can see that there is a significant violation to spherical symmetry in 3-dimensional charge profile as our expectation.

Using Lienard-Wiechert potential, we can calculate the spatial distribution of the electromagnetic

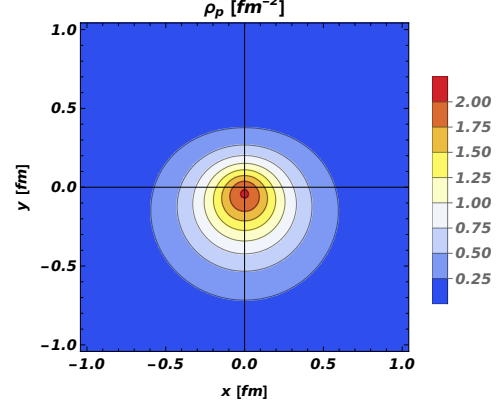


FIG. 1: Plane charge density in a proton polarized along $+x$ direction.

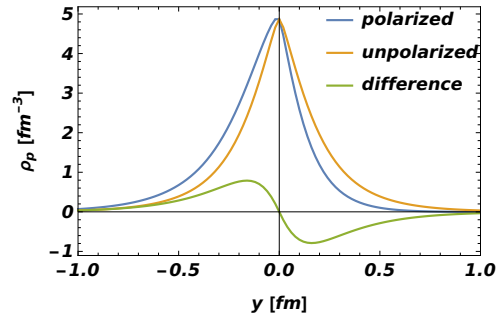


FIG. 2: The 3-dimensional charge profiles in an unpolarized proton (orange curve), and a proton polarized along $+x$ (blue curve) as function of y at $x = 0$ and $z = 0$.

field generated by a single flying polarized proton.

$$\begin{aligned} eE(t, \mathbf{r}) &= \frac{e^2}{4\pi} \sum_n Z_n(\mathbf{R}) \frac{\mathbf{R}_n - \mathbf{R}_n v_n}{(\mathbf{R}_n - \mathbf{R}_n \cdot \mathbf{v}_n)^3} (1 - v_n^2) \\ eB(t, \mathbf{r}) &= \frac{e^2}{4\pi} \sum_n Z_n(\mathbf{R}) \frac{\mathbf{v}_n \times \mathbf{R}_n}{(\mathbf{R}_n - \mathbf{R}_n \cdot \mathbf{v}_n)^3} (1 - v_n^2) \end{aligned} \quad (7)$$

here Z_n is the n^{th} particle charge number, v_n is its velocity. $\mathbf{R}_n = \mathbf{r} - \mathbf{r}_n$ is the relative position of the field point \mathbf{r} and the source point \mathbf{r}_n which is the n^{th} particle at the position with a delay time of $t_n = t - |\mathbf{r} - \mathbf{r}_n|$ [11].

We set the proton polarized along $+x$ axis still, and flying with a RHIC energy scale (100 GeV) along $+z$ direction. $t = 0$ is set as the proton just

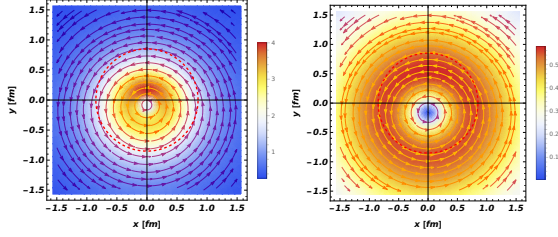


FIG. 3: The distribution of magnetic field B on plane with $z = 0$ (left panel), and $z = 1/\gamma \text{fm}$ (right panel) at $t = 0$. A red circle with $r = 0.85 \text{fm}$ is shown together, which is typical radii of proton.

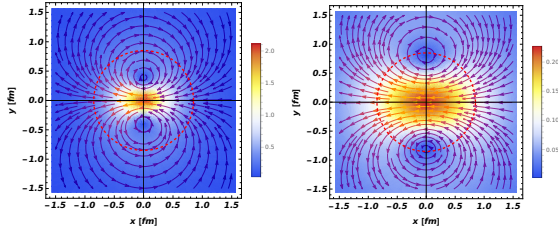


FIG. 4: The distribution of magnetic field difference ΔB on plane with $z = 0$ (left panel), and $z = 1/\gamma \text{fm}$ (right panel) at $t = 0$. A red circle with $r = 0.85 \text{fm}$ is shown together, which is typical radii of proton.

flying through origin of coordinate $z = 0$. Shown in Fig3 is the magnetic field produced by this polarized proton at $t = 0$. Left panel of it showed the vector stream (vector) and strength (color) on plane with $z = 0$, while right panel showed them on plane with $z = 1/\gamma \text{fm}$ with a Lorentz factor $\gamma = E/m_p$.

To compare the magnetic field produced by polarized and unpolarized proton, we defined $\Delta B = B_{pol} - B_{unpol}$. The results are shown in Fig4. We can see that the intensity of ΔB is same order of the strength of B within the circle of proton size, which will be the overlap region in small collision system p+A.

So, let's move from a flying single polarized proton to small collision system $p^\uparrow + \text{Au}$ at RHIC energy $\sqrt{s} = 200 \text{GeV}$. The collision geometry is set as the momentum of proton being $+z$ direction, while the Au nuclei being $-z$ direction. And the polarization is

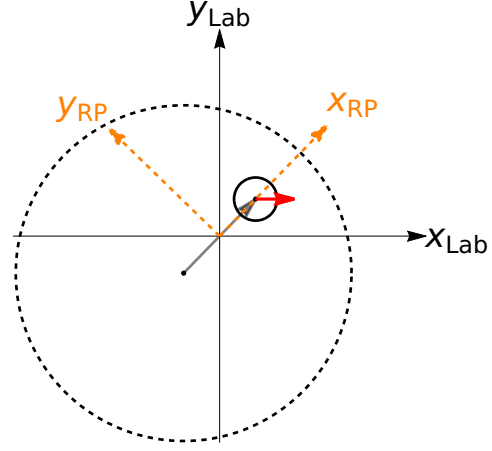


FIG. 5: An Illustration of collision geometry of $p^\uparrow + \text{Au}$ with $\Phi_{RP} \neq 0$.

fixed as $+x$ direction. Impact parameter is defined as the vector point from center of Au to center of proton. Since the azimuthal angle of reaction plane Φ_{RP} is random in each event, we showed an illustration of one event with $\Phi_{RP} \neq 0$ in Fig5. In our following calculation, just four collision geometry schemes are investigated, with $\Phi_{RP} = 0, \pi/2, \pi$, and $3\pi/2$ respectively, illustrated in Fig6.

Then HIJING model [30, 31] is employed to simulate the p+A collision process event by event in each collision scheme. In our calculation of electromagnetic fields, the 3-D unsymmetrical charge profile is used for the transversely polarized projectile proton, and 3-D symmetrical charge profile is used for nucleons in target Au.

Our results of electromagnetic fields on the center of overlap region averaged over events are shown in Fig6 for the four schemes. Components of B and E are projected into frame of event plane. So we can see that the value of B_y is always negative as our expectation.

In order to get the CME signal we calculated correlator as Eq8, here Φ_2 is the azimuthal angle of event plane which is determined by all participants nucleons in each event[32]. Although the difference between Φ_{RP} and Φ_2 is small, the correlator as Eq8

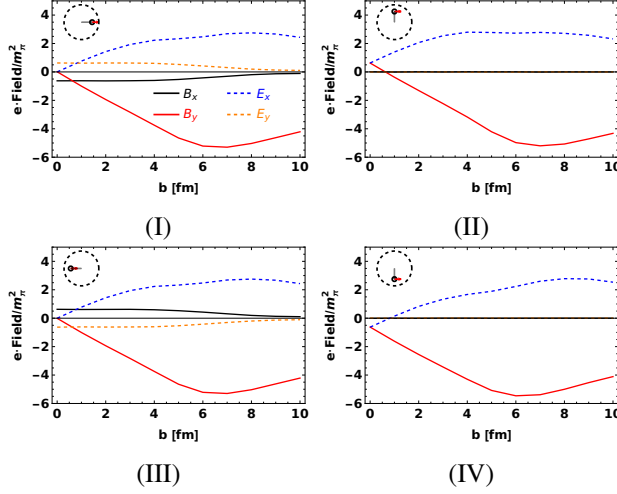


FIG. 6: The strength of electromagnetic fields B_x , B_y , E_x , and E_y as function of impact parameter b in four collision geometry schemes.

is more convenient to compare with possible future experiment data .

$$\Delta\gamma_{\text{CME}} \propto B^2 \cdot \cos[2(\Phi_B - \Phi_2)], \quad (8)$$

The results of the correlators as function of impact parameter b in the four schemes are shown in Fig7. In each scheme, the correlator is not zero at small b because of the fluctuation of \mathbf{B} is not vanished in each event. Especially, we noticed that there is a significant difference between scheme II and scheme IV. These two schemes are corresponding to the azimuthal angle of impact parameter b lying on the $+y$ and $-y$ sectors respectively in lab frame. People can distinguish these two schemes in experiment with Zero Degree Calorimeters on RHIC.

It is more obvious to see the difference of CME correlators between scheme II and IV $\Delta\gamma_{\text{CME II}} - \Delta\gamma_{\text{CME IV}}$, shown in Fig8. The difference in the two schemes increase with impact parameter, and reach a same order of Au+Au collision. So, if QGP is produced in small collision system, and CME exist here, its contribution to correlator will be much different between scheme II and scheme IV. On the other hand, background flow effects can be canceled completely even if it's not negligible when we check

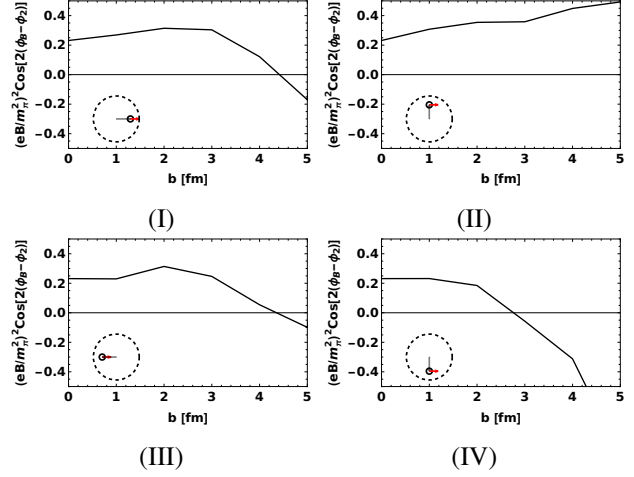


FIG. 7: $B^2 \cdot \cos[2(\Phi_B - \Phi_2)]$ as function of impact parameter b in four collision geometry schemes.

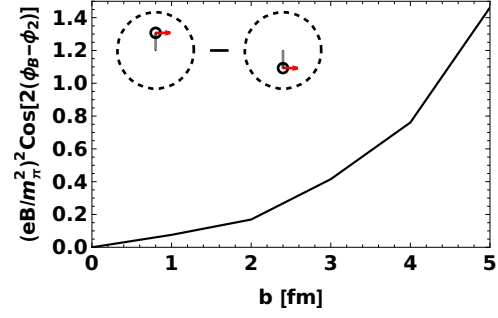


FIG. 8: Difference of $B^2 \cdot \cos[2(\Phi_B - \Phi_2)]$ between scheme II and scheme IV, as function of impact parameter b .

the difference between experiment data of scheme II and scheme IV.

$$\begin{aligned} \Delta\gamma_{\text{II}} - \Delta\gamma_{\text{IV}} &\propto (\Delta\gamma_{\text{CME II}} + \Delta\gamma_{\text{BG II}}) \\ &\quad - (\Delta\gamma_{\text{CME IV}} + \Delta\gamma_{\text{BG IV}}) \\ &\propto \Delta\gamma_{\text{CME II}} - \Delta\gamma_{\text{CME IV}} \end{aligned} \quad (9)$$

So this $p^\dagger + A$ small collision system can provide us an ideal method to check the contribution of CME.

The authors acknowledge the support from the National Natural Science Foundation of China (No. 12075094). The computation is completed in the HPC Platform of Huazhong University of Science and Technology. We thank Prof. Qing-Hua Xu for his helpful discussion.

-
- [1] D. Kharzeev, R. D. Pisarski, and M. H. G. Tytgat, *Phys. Rev. Lett.* **81**, 512 (1998), [arXiv:hep-ph/9804221 \[hep-ph\]](#).
 - [2] D. Kharzeev, *Phys. Lett.* **B633**, 260 (2006), [arXiv:hep-ph/0406125 \[hep-ph\]](#).
 - [3] D. E. Kharzeev, L. D. McLerran, and H. J. Warringa, *Nucl. Phys.* **A803**, 227 (2008), [arXiv:0711.0950 \[hep-ph\]](#).
 - [4] K. Fukushima, D. E. Kharzeev, and H. J. Warringa, *Phys. Rev.* **D78**, 074033 (2008), [arXiv:0808.3382 \[hep-ph\]](#).
 - [5] D. E. Kharzeev, J. Liao, S. A. Voloshin, and G. Wang, *Prog. Part. Nucl. Phys.* **88**, 1 (2016), [arXiv:1511.04050 \[hep-ph\]](#).
 - [6] Y.-C. Liu and X.-G. Huang, *Nucl. Sci. Tech.* **31**, 56 (2020), [arXiv:2003.12482 \[nucl-th\]](#).
 - [7] J. Rafelski and B. Muller, *Phys. Rev. Lett.* **36**, 517 (1976).
 - [8] V. Skokov, A. Yu. Illarionov, and V. Toneev, *Int. J. Mod. Phys.* **A24**, 5925 (2009), [arXiv:0907.1396 \[nucl-th\]](#).
 - [9] A. Bzdak and V. Skokov, *Phys. Lett.* **B 710**, 171 (2012), [arXiv:1111.1949 \[hep-ph\]](#).
 - [10] V. Voronyuk, V. D. Toneev, W. Cassing, E. L. Bratkovskaya, V. P. Konchakovski, and S. A. Voloshin, *Phys. Rev. C* **83**, 054911 (2011), [arXiv:1103.4239 \[nucl-th\]](#).
 - [11] W.-T. Deng and X.-G. Huang, *Phys. Rev. C* **85**, 044907 (2012), [arXiv:1201.5108 \[nucl-th\]](#).
 - [12] W.-T. Deng and X.-G. Huang, *Phys. Lett. B* **742**, 296 (2015), [arXiv:1411.2733 \[nucl-th\]](#).
 - [13] G. Inghirami, L. Del Zanna, A. Beraudo, M. H. Moghaddam, F. Becattini, and M. Bleicher, *Eur. Phys. J. C* **76**, 659 (2016), [arXiv:1609.03042 \[hep-ph\]](#).
 - [14] L. Yan and X.-G. Huang, (2021), [arXiv:2104.00831 \[nucl-th\]](#).
 - [15] S. A. Voloshin, *Phys. Rev. C* **70**, 057901 (2004), [arXiv:hep-ph/0406311](#).
 - [16] J. Błoczyński, X.-G. Huang, X. Zhang, and J. Liao, *Phys. Lett. B* **718**, 1529 (2013), [arXiv:1209.6594 \[nucl-th\]](#).
 - [17] J. Błoczyński, X.-G. Huang, X. Zhang, and J. Liao, *Nucl. Phys. A* **939**, 85 (2015), [arXiv:1311.5451 \[nucl-th\]](#).
 - [18] H.-J. Xu, X. Wang, H. Li, J. Zhao, Z.-W. Lin, C. Shen, and F. Wang, *Phys. Rev. Lett.* **121**, 022301 (2018), [arXiv:1710.03086 \[nucl-th\]](#).
 - [19] L. Adamczyk *et al.* (STAR), *Phys. Rev.* **C89**, 044908 (2014), [arXiv:1303.0901 \[nucl-ex\]](#).
 - [20] F. Wang and J. Zhao, *Phys. Rev.* **C95**, 051901 (2017), [arXiv:1608.06610 \[nucl-th\]](#).
 - [21] N. N. Ajitanand, R. A. Lacey, A. Taranenko, and J. M. Alexander, *Phys. Rev.* **C83**, 011901 (2011), [arXiv:1009.5624 \[nucl-ex\]](#).
 - [22] A. Bzdak, *Phys. Rev.* **C85**, 044919 (2012), [arXiv:1112.4066 \[nucl-th\]](#).
 - [23] J. Zhao, H. Li, and F. Wang, (2017), [arXiv:1705.05410 \[nucl-ex\]](#).
 - [24] Z.-W. Zhang, X.-Z. Cen, and W.-T. Deng, *Chin. Phys. C* **46**, 084103 (2022), [arXiv:2108.09910 \[hep-ph\]](#).
 - [25] C. E. Carlson and M. Vanderhaeghen, *Phys. Rev. Lett.* **100**, 032004 (2008), [arXiv:0710.0835 \[hep-ph\]](#).
 - [26] G. A. Miller, *Ann. Rev. Nucl. Part. Sci.* **60**, 1 (2010), [arXiv:1002.0355 \[nucl-th\]](#).
 - [27] J. J. Kelly, *Phys. Rev. C* **66**, 065203 (2002), [arXiv:hep-ph/0204239](#).
 - [28] W. M. Alberico, S. M. Bilenky, C. Giunti, and K. M. Graczyk, *Phys. Rev. C* **79**, 065204 (2009), [arXiv:0812.3539 \[hep-ph\]](#).
 - [29] J. Arrington, W. Melnitchouk, and J. A. Tjon, *Phys. Rev. C* **76**, 035205 (2007), [arXiv:0707.1861 \[nucl-ex\]](#).
 - [30] M. Gyulassy and X.-N. Wang, *Comput. Phys. Commun.* **83**, 307 (1994), [arXiv:nucl-th/9502021](#).
 - [31] W.-T. Deng, X.-N. Wang, and R. Xu, *Phys. Rev. C* **83**, 014915 (2011), [arXiv:1008.1841 \[hep-ph\]](#).
 - [32] W.-T. Deng, Z. Xu, and C. Greiner, *Phys. Lett. B* **711**, 301 (2012), [arXiv:1112.0470 \[hep-ph\]](#).